Thermal Denaturation Studies of Collagen by Microthermal Analysis and Atomic Force Microscopy

Laurent Bozec[†*] and Marianne Odlyha[‡]
[†]Biomaterials and Tissue Engineering, Eastman Dental Institute, University College London, London, United Kingdom; and [‡]Institute of Structural and Molecular Biology, Department of Biological Sciences at Birkbeck College, University of London, London, United Kingdom

ABSTRACT The structural properties of collagen have been the subject of numerous studies over past decades, but with the arrival of new technologies, such as the atomic force microscope and related techniques, a new era of research has emerged. Using microthermal analysis, it is now possible to image samples as well as performing localized thermal measurements without damaging or destroying the sample itself. This technique was successfully applied to characterize the thermal response between native collagen fibrils and their denatured form, gelatin. Thermal transitions identified at (150 ± 10)°C and (220 ± 10)°C can be related to the process of gelatinization of the collagen fibrils, whereas at higher temperatures, both the gelatin and collagen samples underwent two-stage transitions with a common initial degradation temperature at (300 ± 10)°C and a secondary degradation temperature of (340 ± 10)°C for the collagen and of (420 ± 10)°C for the gelatin, respectively. The broadening and shift in the secondary degradation temperature was linked to the spread of thermal degradation within the gelatin and collagen fibrils matrix further away from the point of contact between probe and sample. Finally, similar measurements were performed inside a bone resorption lacuna, suggesting that microthermal analysis is a viable technique for investigating the thermomechanical response of collagen for in situ samples that would be, otherwise, too challenging or not possible using bulk techniques.

INTRODUCTION

Although the biophysics of tendons and bones has been studied for decades using several different microscopic approaches, there has been a resurgence of interest as novel techniques such as scanning probe microscopy have become available in this area of research. Collagen, the most abundant protein in mammals, is a fibrous structural protein and provides an intriguing example of a hierarchical biological nanomaterial. The collagen molecule consists of triple helical tropocollagen molecules that have highly conserved lengths of L ~300 nm, roughly 1.5 nm in diameter. Staggered arrays of collagen molecules form fibrils, which arrange to form collagen fibers (1–5). Collagen plays an important structural role in many biological tissues, such as, for example, in tendon, bone, teeth, cartilage, and the cardiovascular system.

There has been a recent report suggesting that collagen may be unstable at room temperature, leading to the conclusion that this protein, the main constituent of the human body and skeleton, may appear in a denatured state under normal physiological conditions (6). Collagen is also the main component of parchment which in the form of archival material bears the testimony of recorded cultural history and so necessitates its preservation. This relies on knowledge of the hydrothermal stability of the fibers of historical parchments. Studies in previous projects (7,8) have shown that fibers of some historical parchments with low hydrothermal stability are transformed into a gelatin structure by immediate contact with water at room temperature. Thus, studies for characterizing the extent of gelatinization of parchment fibers, used on collagen in its dry state, will prevent irreversible damage which can occur during storage and conservation treatment. In an attempt to understand the thermomechanical properties of this structural molecule and its higher order hierarchical arrangements, which exist in the collagen fibril, a study was carried out using what we believe to be a novel approach—i.e., microthermal analysis, which has been mainly used for analysis of polymers.

Microthermal analysis was developed by Hammiche et al. (9,10) following the original work by Majumdar et al. (11,12) in scanning thermal microscopy. This technique combines the capabilities of atomic force microscopy (AFM) with those of thermomechanical analysis, differential thermal analysis, and analytical pyrolysis (13). These modes of operation are achieved by replacing the standard AFM probe by a thermally controlled AFM probe (13). Previous thermoanalytical studies of collagen denaturation have been performed using bulk analytical techniques such as differential scanning calorimetry (DSC) (14–16), as it has not been possible to perform localized thermal measurements and minimize the volume of materials being sampled.

However, using microthermal analysis, thermal analysis measurements can be carried out by placing a thermally controlled AFM probe on a sample and by recording its thermomechanical response as the probe temperature is increased. As the samples undergo thermal transitions, changes in probe deflection (μm) are recorded as a function of the probe temperature. This known as localized

Submitted November 12, 2010, and accepted for publication April 14, 2011.

*Correspondence: l.bozec@ucl.ac.uk

Editor: Daniel J. Muller.

0006-3495/11/07/0228/9 $2.00

doi: 10.1016/j.bpj.2011.04.033

thermomechanical analysis (L-TMA) (17). The key advantage of this approach over conventional DSC or TMA techniques is that the measurements are performed directly on the sample over a region defined by the contact area between the probe and sample (typically ~20 μm diameter for a Wollaston wire probe) and therefore do not require destroying the sample entirely while performing the measurement. This approach presents advantages in studies where samples size is limited and where spatially resolved measurements are required.

In this article, microthermal analysis was used to characterize the thermal transitions of native tendon collagen and that of its denatured form, gelatin, with the view to provide a thermomechanical fingerprint response for both native and denatured collagen. This initial approach was complemented by a further study of the thermomechanical characterization of collagen present within resorption lacunae. The aim of the research presented here is to demonstrate that measurements performed locally using a thermally controlled AFM probe provide spatially resolved information which is inaccessible via standard bulk thermoanalytical techniques.

MATERIAL AND METHODS

Native collagen

Segments from rat-tails were obtained from rats sacrificed for other experiments. Bundles of fibrils were subsequently pulled out of the tails using fine tweezers. The resulting bundles of fibrils were then stored in phosphate buffer saline at 4°C. For the topological and thermomechanical measurements, single fibrils were drawn out of fibril bundles followed by a thorough rinsing in ultra-high quality (UHQ) water. The fibrils were then physisorbed onto a glass slide using a gentle N_2 flow to ensure that the fibrils were immobilized, which is a prerequisite for AFM measurements. For the hydrated measurements, fibrils were prepared as for imaging (physisorption on glass), but were rehydrated for 5 min using UHQ water as performed in previous experiments (18). Excess water was subsequently drained away and measurements were performed within the next minute to ensure that the fibrils remained hydrated.

Gelatin

Gelatin samples were prepared by thermal denaturation of the collagen fibrils in a microblock at 70°C for 5 min in UHQ water before being centrifuged very gently and stored at 4°C. A 40-μL droplet of the gelatin preparation was then smeared and dried on a glass slide for imaging, whereas a larger droplet (~200–300 μL) was dried onto the glass slide for the thermomechanical measurements.

Dentine chips

Dentine chips were prepared from elephants' tusks (obtained from HM Customs UK, United Kingdom) by cutting very thin slices using a diamond across the tusk. The slices were then washed with water to remove loose materials from the cutting process, and subsequently punch-holed to create chips of ~5 mm in diameter. Once obtained, the chips were polished using 3-mm paper before being sterilized. Furthermore, to access the collagen matrix on the dentine chip, osteoclasts were isolated from 5-day-old rabbits, and cultured on these slices as described by Boyde et al. (19) and Chambers et al. (20).

Briefly, osteoclasts were mechanically harvested from humeri, tibiae, and femura, cultured on dentine slices. After 30 min of incubation, unattached cells were removed by washing with medium and the samples were cultured in Dulbecco's modified Eagle's medium supplemented with 10% fetal calf serum (Gibco BRL, Paisley, Scotland, UK), pH 7.0, 5% CO_2/95% air, at 37°C for 24 h before stopping the cultures. Once sufficient resorption pits could be observed using either immunostaining and confocal microscopy or electron microscopy, samples were rinsed using UHQ water and dried off by a gentle flow of N_2 (21).

Atomic force microscopy

For the topological assessment of the samples, a Dimension-Nanoscope IV (Bruker, Santa Barbara, CA) atomic force microscope was operated in contact mode using DNPS probes. A typical scan rate of 2 Hz was used, while the deflection setpoint was reduced to minimize the force applied onto the sample. Both deflection and topography images were recorded.

Microthermal analysis

For the thermal measurements, a modified Explorer (Bruker) force microscope was operated using the microthermal analysis user interface (TA Instruments, New Castle, DE). To perform L-TMA measurements using the microthermal analysis user interface, a thermally controlled AFM probe is brought into contact with the sample by applying a nominal load constant for all samples studied (4 μN). As the temperature ramp was applied to the thermal probe (the AFM probe behaving like a localized heat source), the deflection of the probe was monitored accordingly. Any thermal transition occurring within the sample and inducing a change in its thermomechanical properties was recorded as a variation in the probe deflection. The probe consists of a Wollaston wire (5 μm in diameter) shaped into a loop, as described elsewhere (22). The probe was calibrated using polymer standards before use with a ± 10°C standard error (23). A typical temperature ramp of 20°C/s was used for all subsequent thermal measurements from room temperature to 500°C, with a cleaning cycle to 650°C for 2 s between measurements. All measurements were repeated at different locations (5 or 7) on the samples to ensure the validity of the measurements. Transitions temperatures were calculated from the L-TMA curves by using the tangent method to calculate the onset temperature of the transitions.

RESULTS AND DISCUSSION

Topological assessment of collagen and gelatin by AFM

To characterize the effect of heat denaturation on the topology of the collagen fibril samples, AFM imaging of the fibrils originating from the tendon fascicle was carried out. In Fig. 1 *a*, the collagen fibrils were tested as prepared on a glass slide, whereas in Fig. 1 *b*, the collagen fibrils were subjected to a heat cycle before being deposited on a glass slide. In Fig. 1 *a*, long fibrils with the characteristic annular periodicity along the length of the fibril, known as D-banding, can be observed. This topology of the collagen fibrils is well known and can be associated with the native state of the fibrils (4,24,26). The width of D-banding periodicity has been extensively studied using AFM, having a value varying between 67 and 69 nm, depending on the hydration of the fibril. In our case, the D-banding was found to be $D = 67.8 \pm 2.4$ nm ($N = 220$).

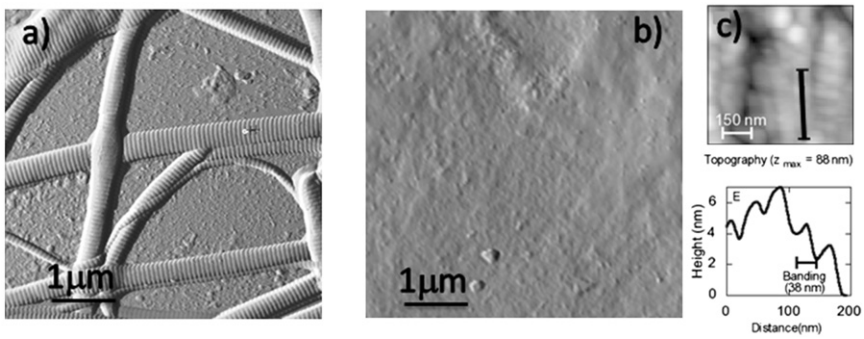

FIGURE 1 Atomic force microscopy deflection images of (*a*) native collagen fibrils from rat tails' tendon on glass slide displaying a 67-nm banding periodicity, (*b*) gelatinized collagen fibrils prepared on glass slide, and (*c*) 38-nm banding fibrillar periodicity observed on gelatinized collagen sample.

Another interesting feature observable in Fig. 1 *a* is the variation in the fibril diameter ranging from (50 ± 4) nm to >(350 ± 4) nm. The distribution of these diameters is not normally distributed over the range, and a bimodal distribution with two maxima at (75 ± 12) nm and (250 ± 120) nm, respectively, could be plotted. This bimodal distribution is in agreement with other studies and can be associated with the maturity of the fibrils and their mechanical loading cycle (27–29). In Fig. 1 *b*, the product of thermal denaturation of collagen fibrils, gelatin, has been imaged. The gelatin appears as a smooth glassy layer that is not reminiscent of its former topology as described in Fig. 1 *a*. The apparent lack of fibrillar structure indicates a complete loss of the well-established ultrastructure of collagen fibrils, and suggests that the collagen has been entirely structurally degraded during the heating cycle.

Upon denaturation, collagen fibrils undergo several conformational changes caused by the breaking of different cross-links present at the intermolecular level such as the nonenzymatic glycosylation of lysine and hydroxylysine residues and at the intramolecular level such as the disulphide bridges (30). Furthermore, the H-bonded water used to stabilize the collagen molecule is released (31), leading to the collapse of the triple helix structure of the molecules. The end result of the thermal denaturation of collagen is random fragmentation of the collagen fibril and molecule, due to the loss of those cross-links that are necessary to stabilize the collagen fibril ultrastructure (32). It is, however, possible to observe some fibrillar structure in one studied area of the gelatin sample, as displayed in Fig. 1 *c*. Although the collagen was heated to 70°C for 5 min, a rare case of fibril displaying a repetitive periodicity was observed.

As shown in Fig. 1 *c*, the periodicity of the fibril was measured as $D = (38 \pm 10)$ nm. A similar reduction in the banding periodicity was also recorded on rat-tail collagen heated to 100°C for 15 min by de Groot (33). One plausible explanation for this apparent reduction in banding periodicity would be that before the breaking of the cross-links as suggested before, the triple helix ultrastructure undergoes local unfolding at a thermally less stable domain, as suggested by Miles et al. (34). According to the authors, such a domain is located in the gap region of the collagen ultrastructure. Local unfolding in the gap region would reduce the banding periodicity, while maintaining the collagen fibril ultrastructure intact.

Collagen denaturation in hydrated environment by microthermal analysis

To understand the effect of an increase of temperature on native collagen fibril, L-TMA measurements were initially performed on a hydrated collagen sample. Fig. 2 presents L-TMA curves obtained by performing such measurement on hydrated collagen fibrils. As the temperature of the probe increases, the probe deflection remains constant until the onset of the transition at (58 ± 10)°C and the main transition occurs at $T_{coll1} = (65 \pm 10)$°C. The main transition corresponds to the process of gelatinization of collagen in a hydrated environment and is caused by the breaking of internal cross-links. The onset temperature at (58 ± 10)°C is explained by conformational changes occurring within the fibrils before the main denaturation transition, such as partial shrinkage of the fibrils. This shrinkage would also explain the initial shift in the probe deflection as seen in Fig. 2 and possibly the reduction in the D-banding periodicity as found in Fig. 1 *c*. This shrinkage phenomenon was also reported by Lin et al. (35) using a second harmonic generation microscopy approach.

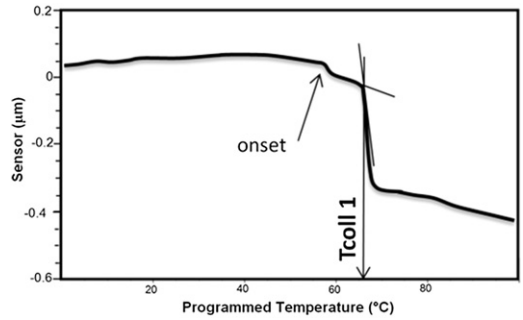

FIGURE 2 Localized thermomechanical analysis (L-TMA) curves recorded on hydrated collagen fibrils, displayed as sensor (probe deflection) versus program temperature (probe temperature). Onset of transition occurs at 58°C and the main denaturation transition occurs at 65°C.

One of the limitations of microthermal analysis is that the thermal probe needs to come into physical contact with the sample and therefore limits the range of sample that can be used for solids or near-solids. Gelatin is by definition a random fragmentation of collagen fibrils in aqueous environment, and therefore performing L-TMA measurement on hydrated gelatin would be difficult as the thermal probe is not able to make contact with the sample surface due to the hydrogel structure of gelatin. Moreover, because the measurements are not performed inside a closed sample chamber, an increase in the probe temperature toward 100°C would dry the sample before any thermal events could be detected. In the case of the hydrated collagen, the increase in probe temperature past the denaturation temperature $T_{coll1} = (65 \pm 10)$°C induces a phase change in collagen from solid to liquid (or hydrogel) as inter- and intramolecular cross-links are broken.

Another possible limitation of this approach is the high heating rate used during the measurement. Heating rates values ranging from 10 to 25°C/s have been used by Pollock and Hammiche (13), allowing for the measurements to be performed in a few minutes. Reducing that heating rate to a few degrees/s would impact upon the *x-y* scanner stability of the AFM because measurements would take several hours and mechanical drift would displace the probe from its original point of contact with the sample (36). However, it is known that collagen denaturation behavior varies with the heating rate applied, as demonstrated by Miles and Bailey (30) using differential scanning calorimetry to denature collagen. They demonstrated that the temperature at which denaturation occurs is not a constant but increases approximately linearly with the logarithm of the heating rate.

Collagen denaturation in dry environment by microthermal analysis

Although collagen is mostly commonly studied in physiological conditions, it is still relevant to investigate the effect of an increase of temperature in a dry environment, as dry collagen is used in a wide variety of products and heritage objects (7,37). Thus, L-TMA measurements were also performed on dry collagen fibrils, and on their gelatinized form, as shown in Fig. 3.

Collagen fibrils (dry)

In the case of native collagen (Fig. 3, *solid line*), the fibrils undergo thermal expansion up to 150°C caused by the swelling of the collagen fibrils. The transition temperature, $T_{coll2} = (150 \pm 10)$°C, is associated with the evaporation of residual, strongly H-bonded water responsible for the stability of the triple helix conformation of collagen macromolecules. Direct evidence of the existence and coordination of the bound water in these proteins structure has been verified using various structure-sensitive techniques including infrared spectroscopy (38), NMR spectroscopy (39,40),

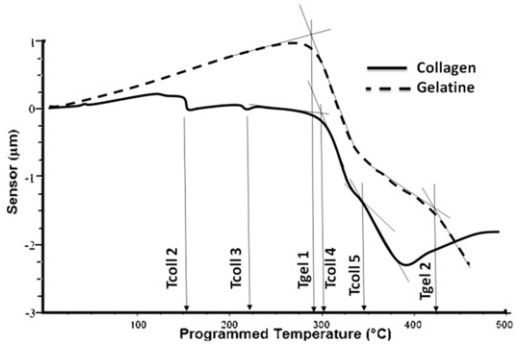

FIGURE 3 L-TMA curves recorded on dry collagen fibrils (*solid line*) and dry gelatin (*dotted line*) displayed as sensor (probe deflection) versus program temperature (probe temperature). The transitions T_{coll} and T_{gel} correspond, respectively, to the thermal events occurring in the dry collagen and the dry gelatin.

circular dichroism (41), and x-ray and neutron diffraction (42,43). As the probe temperature is increased, a second transition is detected at $T_{coll3} = (220 \pm 10)$°C which is associated with conformational changes of the collagen molecules from a triple helix structure to random coil (44,45). This transition has often been referred as the first-order transition of the denaturation of dehydrated collagen.

As reported previously, this transition temperature shifts toward lower temperature in solutions (such as UHQ water) as observed previously with T_{coll1}. The difference in the probe deflection between T_{coll2} and T_{coll3} indicates that thermal denaturation in a dry environment depends strongly on the degree of hydration as suggested by Privalov and Tiktopulo (46). This denaturation behavior for native dry collagen is in a good agreement with the data reported by Friess and Lee (47) and Pietrucha (48). Using DSC, Samouillan et al. (49) have observed an endothermic peak at ~226°C in bovine tendon. On increasing the temperature above 300°C, degradation of the material occurs. In Fig. 3, the two transitions $T_{coll4} = (305 \pm 10)$°C and $T_{coll5} = (345 \pm 10)$°C, which represent the two-stage degradation of the collagen fibrils, are shown.

To understand this two-stage transition, topographical images were recorded on a collagen matrix after such a measurement was performed. Fig. 4 *a* presents the imprint left by the thermal probe on the bundle of collagen fibrils where an L-TMA measurement was previously made. More images were recorded close to the L-TMA imprint site, where a gelatinized area could be observed in the area immediately surrounding the imprint, as shown in Fig. 4 *c*. However, collagen fibrils with noticeable D-banding periodicity could be observed at a distance (15 ± 4) μm away from the initial contact point between probe and sample. If the probe temperature ramp is stopped before $T_{coll5} = (345 \pm 10)$°C, one cannot observe any propagation of the thermal degradation in the collagen fibril beyond the initial contact area between probe and sample, as shown in Fig. 4, *e* and *d*.

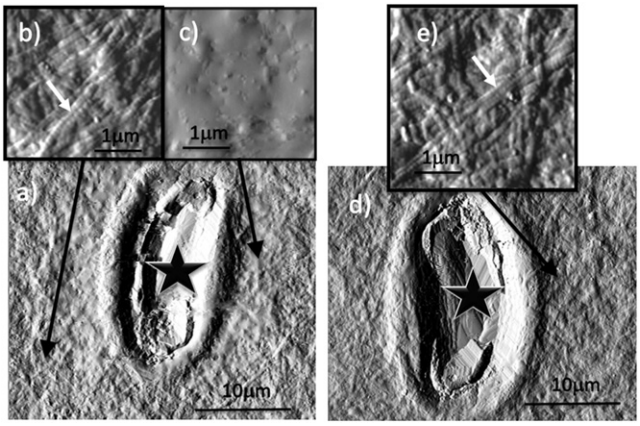

FIGURE 4 (*a* and *d*) Oblong probe imprints (*star*) left on the sample after performing an L-TMA with temperature ramp stopped, respectively, at 500°C (*a*) and 300°C (*d*). (*b*) Intact collagen matrix at a distance of 15 μm away from the border of the imprint, (*c*) denatured collagen matrix at the vicinity of the imprint, and (*e*) intact collagen matrix adjacent to the probe imprint.

In that case, the probe temperature ramp was stopped at 300°C, which was sufficient to degrade only the collagen situated directly beneath the probe. Intact fibrils displaying a D-banding periodicity can be observed directly adjacent to the L-TMA imprint site. Because the thermal probe consists of a 5-μm-diameter wire shaped into a loop, the contact area between the probe and sample cannot be considered as a discrete contact point but, rather, as an oblong-shaped contact area (~10 × 20 μm). The spread of the degradation will not be uniform from the original area of contact between probe and sample, and thus the pattern for the spreading of that degradation will be a function of the initial contact between probe as sample, as discussed by Wang (50) and even more recently by Fenwick et al. (51).

Gelatin (dry)

In the case of the gelatin, (Fig. 3, *dotted line*), no thermomechanical transitions were recorded before the transition temperature $T_{gel1} = (290 \pm 10)$°C. The presence of a significant thermal expansion at temperatures below T_{gel1} is not specific to gelatin as successive measurements were inconclusive to explain the presence or not of surface expansion in L-TMA traces of gelatin. This may be due to the structural heterogeneity of gelatin at locations where measurements were performed. The reason for the lack of thermomechanical transition before T_{gel1} is due to the fact that the collagen has already undergone similar transitions while being processed into gelatin. As the probe temperature reaches $T_{gel1} = (290 \pm 10)$°C, the main degradation of gelatin occurs as indicated by the probe deflection. In a similar manner to collagen, gelatin undergoes two-stage degradation as the probe temperature is further increased. The propagation of the degradation within the sample occurs at $T_{gel2} = (420 \pm 10)$°C.

Two stage-degradation: thermal markers for structural ordering

As the probe temperature is ramped up to (300 ± 10)°C, both the gelatin and the collagen samples undergo their first phase of degradation. During that phase, the probe has supplied enough heat to the sample to degrade the materials present at the contact point between probe and sample. This transition temperature seems unrelated to the structural difference between the collagen and the gelatin, and hence may not be used as a marker for structural ordering. However, the shift in the temperature of the second degradation phase can be associated with the structural properties of the sample itself, and can be used as a marker for extent of gelatinization of the sample.

During the localized thermomechanical measurement, as the temperature ramp is applied to the thermal probe, the volume of material being degraded increases due to heat diffusion occurring within the sample. This was modeled recently by Fenwick et al. (51), who showed that effect by finite-element method simulations. The critical parameter involved in the spreading of the heat within the sample is the thermal conductivity of the sample, which is the same in the case of collagen and gelatin (respectively, 0.60 W m^{-1} K^{-1} for collagen and 0.62 W m^{-1} K^{-1} for gelatin). Thus, one should expect that both collagen and gelatin would respond in a similar manner to the same applied heat. Experimental results imply that this is not the case, as collagen and gelatin have two very distinct second degradation transitions temperatures: $T_{coll5} = (345 \geq 10)$°C and $T_{gel2} = (420 \pm 10)$°C (Table 1). One hypothesis that may be considered is the presence or not of "ordering" in the collagen or gelatin.

Ordering here can be defined as the presence of organizational structure within the macromolecules complex that is

TABLE 1 Transition temperature obtained from microthermal measurement performed on collagen and gelatin

Sample	Transition temperature (± 10.0)°C		Description
Collagen (hydrated)	T_{coll1}	65	Denaturation temperature of native hydrated collagen.
	T_{coll2}	150	Evaporation of residual, strongly H-bonded water responsible for the stability of the triple helix.
Collagen (dry)	T_{coll3}	220	Conformational changes of the collagen molecules from a triple helix structure to random coil.
	T_{coll4}	305	First stage bulk degradation of dried collagen fibril.
	T_{coll5}	345	Second stage bulk degradation of dried collagen fibril.
Gelatin (dry)	T_{gel1}	290	First stage bulk degradation of dried gelatin.
	T_{gel2}	420	Second stage bulk degradation of dried gelatin.

the collagen fibril. Collagen fibril displays a high level of ordering analogous to crystalline material, whereas gelatin is often described as an amorphous gel, consisting of a fragmentation of the original collagen fibril (52). From a biological structural point of view, crystalline structures are formed by repeating a three-dimensional pattern of molecules. It is known that at a given temperature, heat will travel a shorter distance in the amorphous phase than in the crystalline phase of the same material. Thus, this would explain why the heat diffuses more rapidly in the collagen fibril than in the gelatin, whose second degradation phase occurs at a higher temperature than that of native collagen. Taking this into account, one may use the broadening of the temperature difference to monitor the level of structural ordering in collagen fibrils. By using the difference between the initial degradation temperatures and the secondary propagation temperature, it may also be possible to account for the degree of denaturation present in a given sample, as well as relate that shift in temperature to the degree of cross-linking present in collagen.

Application to mineralized tissue

To further illustrate the advantage of such an approach, localized thermomechanical measurements were also performed on thick slices of ivory-dentine-revealing resorption lacunae, as detailed elsewhere (53,54). The particularity of these resorption lacunae is that the mineral phase has been removed by osteoclastic activity, exposing the collagen matrix present in the ivory slices (21). Before performing the thermomechanical measurements within the resorption lacunae, AFM imaging was carried out directly on a dried cultured dentine slice and especially in the resorption lacunae as presented in Fig. 5 *a*. The lacunae dimensions ranged from 25 to 50 μm in width, between 3- and 7-μm deep and up to several hundreds of microns in length. As mentioned in Bozec et al. (21), the presence of a D-banding periodicity on the fibrils in the lacuna (Fig. 5 *b*) suggests that the resorption process from the osteoclast (cell involved in the renewal process of bones) has not altered significantly the ultrastructure of collagen fibrils.

To further this result, L-TMA measurements were performed within the lacunae to characterize the thermomechanical response of the collagen matrix present. Fig. 5 *c* (*solid line*) presents the localized thermal curve (average of five measurements performed along the same lacuna) obtained as the thermal probe was placed within the lacunae and subsequently ramped up in temperature. A number of transitions can be observed on the curve itself and are summarized in Table 2. Although the sample was initially dried using a flow of dried nitrogen, one can observe a very early thermal transition at (65 $\pm$ 5)°C. This transition corresponds to the denaturation temperature of collagen in hydrated environment as presented in Fig. 2. This indicates that there is some residual water still present within the lacunae although

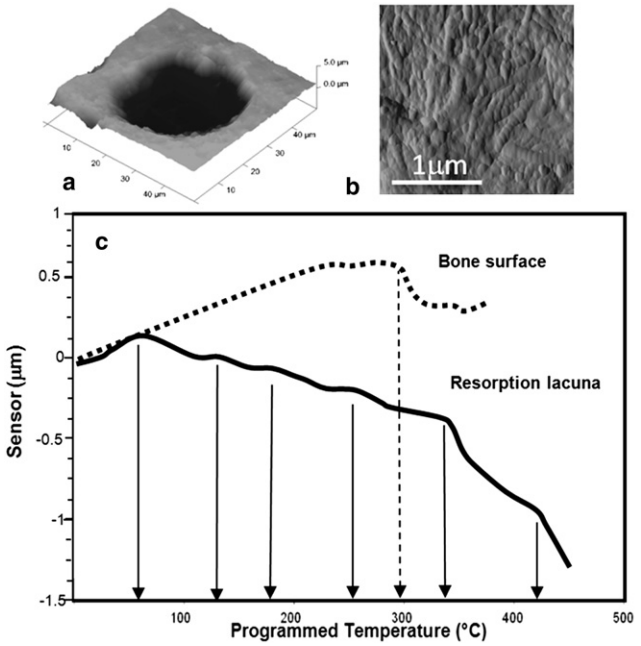

FIGURE 5 (*a*) Three-dimensional AFM image of a typical resorption pit used (5 μm deep) for the L-TMA measurement. (*b*) Presence of intact collagen matrix displaying a clear banding periodicity pattern. (*c*) L-TMA performed in the resorption lacunae.

the sample was dried thoroughly before performing the measurements. One can conclude that the initial matrix present at the bottom of the lacunae consisted initially of "native" or undegraded collagen, which contradicts the older report by Ramachandran and Kartha (2) suggesting that collagen may be unstable at room temperature (6).

The following thermal transitions at (130, 180 $\pm$ 10)°C and (260 $\pm$ 10)°C are related to the denaturation pathways of collagen fibrils in a dry environment, as explained previously in the case of denaturation of native collagen fibrils in the dry state. It has been reported in the literature that calcified collagen will denature at 160°C. Early work by Bonar and Glimcher (55) demonstrated this by using wide- and low-angle x-ray diffraction to investigate the role of the mineral phase in bone in stabilizing both the short-range

TABLE 2 Transition temperature obtained from microthermal measurement performed in a resorption lacuna

Transition temperature ($\pm$ 10.0)°C	Description
65	Denaturation temperature of native hydrated collagen.
130–180	Evaporation of bound water and denaturation of calcified collagen.
260	Conformational changes of the collagen molecules from triple helix structure to random coil.
340	First stage of the collagen matrix degradation.
420	Second stage of gelatin matrix degradation.

(helical) and long-range (the characteristic staggered arrangement of native collagen fibrils) collagen structure against thermal denaturation. As the temperature ramp was further increased, the two-step degradation transitions was observed, at (340 ± 10)°C for the first degradation temperature and (420 ± 10)°C for the second degradation transition, respectively. These transitions correspond to the secondary degradation transitions occurring in native collagen and gelatin, respectively. The results given by this approach suggest that the collagen present at the bottom of a resorption lacuna behaves thermomechanically in a similar manner to native tendon collagen and subsequently to its gelatinized form.

The role of the mineral phase in the thermomechanical response of the probe was not taken into account for this study as the focus was solely on the collagen/gelatin response. It is interesting to note that the presence of minerals did not affect the thermal transition temperatures and direct comparison could be made with transitions occurring in rat-tail tendon in both native gelatinized collagens (55). L-TMA measurements performed on the nonresorbed bone outside the lacuna (Fig. 5 *c*, *dotted line*) do not indicate any early transitions as recorded within the lacuna. In that area of the sample, the bone is fully mineralized and the collagen is surrounded by the mineral phase (hydroxyapatite). A nonspecific thermal expansion can be recorded until a transition temperature of (300 ± 10)°C, which corresponds to the first stage of degradation of dry collagen ($T_{coll4} = (305 \pm 10)$°C).

After that transition, the probe deflection does not indicate any significant melting of the material beneath the probe as it is likely that the mineral phase prevents the probe from sinking into the bone surface. No secondary degradation stage was recorded either because the probe is prevented from sinking further into the sample or because it cannot increase its contact area with the sample. Although the temperature range used for this study may not appear to be physiological, it is still important to understand the effect of such high temperature on mineralized tissue. In the case of bone drilling, for example, cortical bone temperatures >100°C can be recorded if no specific provisions for cooling are made (56,57). This would induce cell necrosis and also partial collagen denaturation.

CONCLUSIONS

This article has, to our thinking, pioneered the application of microthermal analysis to the denaturation studies of collagen in both hydrated and dehydrated conditions. Using this approach, the aim was to understand the thermomechanical response of collagen and gelatin measured using a thermal probe and to correlate it to macroscale measurements. This has enabled the identification of localized thermal denaturation markers for collagen and gelatin at the micron/submicron scale. L-TMA measurements, performed on both collagen fibrils and gelatin, revealed different thermal transitions which could be related to different structural changes occurring in the collagen fibrils during the heating cycle.

At the higher temperature, both collagen and gelatin underwent a two-stage degradation phase in which the first degradation temperature was similar for both samples, but the second degradation temperature was significantly higher in the case of gelatin compared to that of collagen. This result was linked to the spreading of heat away from the initial contact area between probe and sample in both the gelatin and collagen. Experimental results prove that the degradation front within collagen appears at much lower temperatures than that for gelatin. By considering that shift between the two degradation temperatures, it may be possible to fingerprint the response of the collagen sample with a varying degree of structural ordering and varying extent of denaturation.

Although this hypothesis requires more attention, the generic aim of this study was to establish a method of identification of the degraded collagen at the micron/submicron scale. Using this approach, one can make use of the ability of the atomic force microscope to scan and characterize samples locally, without having to either alter the nature of the sample itself though bulk measurement or staining, for example.

Although this study is one of the first analytical characterizations of a biological system using a modified AFM probe, the implications of such a tool for biomedicine and biophysics are numerous. Applications of this protocol will prove useful in fields as varied as dentistry, tissue engineering, and the preservation of heritage collagen-based artifacts such as parchment and leather. The possibility of tracking the degradation of collagenous tissue at the micron/submicron scale opens a new era of understanding for the biophysics of the most abundant protein in the human body.

The authors thank Professor Mike Horton for his help in pioneering the approach used in this manuscript. They also thank Brian Nicholls for his expertise in tissue culture.

REFERENCES

1. Bozec, L., G. van der Heijden, and M. Horton. 2007. Collagen fibrils: nanoscale ropes. *Biophys. J.* 92:70–75.
2. Ramachandran, G. N., and G. Kartha. 1954. Structure of collagen. *Nature.* 174:269–270.
3. Hulmes, D. J. S. 2002. Building collagen molecules, fibrils, and suprafibrillar structures. *J. Struct. Biol.* 137:2–10.
4. Kadler, K. E., D. F. Holmes, …, J. A. Chapman. 1996. Collagen fibril formation. *Biochem. J.* 316:1–11.
5. Hodge, A. J., and J. A. Petruska. 1963. Recent studies with the electron microscope on ordered aggregates of the tropocollagen macromolecule. *In* Aspects of Protein Structure. G. N. Ramachandran, editor. Academic Press, New York. 289–300.
6. Leikina, E., M. V. Mertts, …, S. Leikin. 2002. Type I collagen is thermally unstable at body temperature. *Proc. Natl. Acad. Sci. USA.* 99:1314–1318.

7. Commission, E. 2007. IDAP—Improved Damage Assessment of Parchment. Report No. 18. European Commission, Brussels, Belgium. 120.
8. Larsen, R., D. Poulsen, and M. Vest. 2002. The hydrothermal stability (shrinkage activity) of parchment measured by the micro hot table method (MHT). *In* MicroAnalysis of Parchment (MAP). R. Larsen, editor. Archetype Publications, London, UK. 55–62.
9. Hammiche, A., D. J. Hourston, …, M. Song. 1996. Scanning thermal microscopy: Subsurface imaging, thermal mapping of polymer blends, and localized calorimetry. *J. Vac. Sci. Technol. B.* 14:1486–1491.
10. Hammiche, A., D. M. Price, …, H. M. Pollock. 2000. Two new microscopical variants of thermomechanical modulation: scanning thermal expansion microscopy and dynamic localized thermomechanical analysis. *J. Microsc. Oxf.* 199:180–190.
11. Majumdar, A., J. P. Carrejo, and J. Lai. 1993. Thermal imaging using the atomic force microscope. *Appl. Phys. Lett.* 62:2501–2503.
12. Majumdar, A., J. Lai, …, Z. Shi. 1995. Thermal imaging by atomic force microscopy using thermocouple cantilever probes. *Rev. Sci. Instrum.* 66:3584–3592.
13. Pollock, H. M., and A. Hammiche. 2001. Micro-thermal analysis: techniques and applications. *J. Phys. D Appl. Phys.* 34:R23–R53.
14. McClain, P. E., and E. R. Wiley. 1972. Differential scanning calorimeter studies of the thermal transitions of collagen. Implications on structure and stability. *J. Biol. Chem.* 247:692–697.
15. Knott, L., J. F. Tarlton, and A. J. Bailey. 1997. Chemistry of collagen cross-linking: biochemical changes in collagen during the partial mineralization of turkey leg tendon. *Biochem. J.* 322:535–542.
16. Dai, C. A., Y. F. Chen, and M. W. Liu. 2006. Thermal properties measurements of renatured gelatin using conventional and temperature modulated differential scanning calorimetry. *J. Appl. Polym. Sci.* 99:1795–1801.
17. Price, D. M., M. Reading, …, M. G. Branch. 1999. Localized thermal analysis of a packaging film. *Thermochim. Acta.* 332:143–149.
18. Wenger, M. P. E., M. A. Horton, and P. Mesquida. 2008. Nanoscale scraping and dissection of collagen fibrils. *Nanotechnology.* 19:384006.
19. Boyde, A., N. N. Ali, and S. J. Jones. 1984. Resorption of dentine by isolated osteoclasts in vitro. *Br. Dent. J.* 156:216–220.
20. Chambers, T. J., P. A. Revell, …, N. A. Athanasou. 1984. Resorption of bone by isolated rabbit osteoclasts. *Metab. Bone Dis. Relat.* 5:212.
21. Bozec, L., J. de Groot, …, M. Horton. 2005. Atomic force microscopy of collagen structure in bone and dentine revealed by osteoclastic resorption. *Ultramicroscopy.* 105:79–89.
22. Dinwiddie, R. B., R. J. Pylkki, and P. E. West. 1994. Thermal Conductivity 22. T. W. Tong, editor. Technomics, Lancaster, PA. 668–677.
23. Fischer, H. 2005. Quantitative determination of heat conductivities by scanning thermal microscopy. *Thermochim. Acta.* 425:69–74.
24. Parry, D. A. D., and A. S. Craig. 1984. Growth and development of collagen fibrils in connective tissue. *In* Ultrastructure of the Connective Tissue Matrix. A. Ruggeri and P.M. Motta, editors. Boston, MA. 34–64.
25. Reference deleted in proof.
26. Petruska, J. A., and A. J. Hodge. 1964. Subunit model for tropocollagen macromolecule. *Proc. Natl. Acad. Sci. USA.* 51:871–876.
27. Prockop, D. J., and A. Fertala. 1998. The collagen fibril: the almost crystalline structure. *J. Struct. Biol.* 122:111–118.
28. Currey, J. D. 2002. Bone at the molecular level. *In* Bones: Structure and Mechanics.. Princeton University Press, Princeton, NJ, and Oxford, UK. 3–26.
29. Brown, R. A., M. Wiseman, …, S. N. Nazhat. 2005. Ultrarapid engineering of biomimetic materials and tissues: fabrication of nano- and microstructures by plastic compression. *Adv. Funct. Mater.* 15:1762–1770.
30. Miles, C., and A. Bailey. 1999. Thermal denaturation of collagen revisited. *J. Chem. Sci.* 111:71–80.
31. Fraser, R. D. B., T. P. MacRae, and E. Suzuki. 1979. Chain conformation in the collagen molecule. *J. Mol. Biol.* 129:463–481.
32. Robins, S. P., and A. J. Bailey. 1975. The chemistry of the collagen cross-links. The mechanism of stabilization of the reducible intermediate cross-links. *Biochem. J.* 149:381–385.
33. de Groot, J. 2007. Damage Assessment of Parchment with Scanning Probe Microscopy. University of London, Birkbeck College, London, UK.
34. Miles, C. A., T. V. Burjanadze, and A. J. Bailey. 1995. The kinetics of the thermal denaturation of collagen in unrestrained rat tail tendon determined by differential scanning calorimetry. *J. Mol. Biol.* 245:437–446.
35. Lin, S. J., W. Lo, …, C. Y. Dong. 2006. Prediction of heat-induced collagen shrinkage by use of second harmonic generation microscopy. *J. Biomed. Opt.* 11:34020.
36. Bozec, L. 2002. Near-Field Photothermal Fourier-Transform Infrared Micro-Spectrometry. Lancaster University, Bailrigg, Lancaster, UK, 225.
37. Odlyha, M., C. Theodorakopoulos, …, M.A. Horton. 2009. Fourier transform infra-red spectroscopy (ATR/FTIR) and scanning probe microscopy of parchment. [In Russian]. e-Preservation Science. 6:138–144.
38. Renugopalakrishnan, V., G. Chandrakasan, …, R. S. Bhatnagar. 1989. Bound water in collagen—evidence from Fourier-transform infrared and Fourier-transform infrared photoacoustic spectroscopic study. *Macromolecules.* 22:4121–4124.
39. Liu, W. G., and K. De Yao. 2001. What causes the unfrozen water in polymers: hydrogen bonds between water and polymer chains? *Polymer (Guildf.).* 42:3943–3947.
40. Ernst, J. A., R. T. Clubb, …, G. M. Clore. 1995. Demonstration of positionally disordered water within a protein hydrophobic cavity by NMR. *Science.* 267:1813–1817.
41. Holmgren, S. K., K. M. Taylor, …, R. T. Raines. 1998. Code for collagen's stability deciphered. *Nature.* 392:666–667.
42. Bella, J., B. Brodsky, and H. M. Berman. 1995. Hydration structure of a collagen peptide. *Structure.* 3:893–906.
43. Bella, J., M. Eaton, …, H. M. Berman. 1994. Crystal and molecular structure of a collagen-like peptide at 1.9-Ångstrom resolution. *Science.* 266:75–81.
44. Luescher, M., M. Rüegg, and P. Schindler. 1974. Effect of hydration upon the thermal stability of tropocollagen and its dependence on the presence of neutral salts. *Biopolymers.* 13:2489–2503.
45. Bigi, A., G. Cojazzi, …, M. H. J. Koch. 1987. Differential scanning calorimetry and x-ray-diffraction study of tendon collagen thermal-denaturation. *Int. J. Biol. Macromol.* 9:363–367.
46. Privalov, P. L., and E. I. Tiktopulo. 1970. Thermal conformational transformation of tropocollagen. I. Calorimetric study. *Biopolymers.* 9:127–139.
47. Friess, W., and G. Lee. 1996. Basic thermoanalytical studies of insoluble collagen matrices. *Biomaterials.* 17:2289–2294.
48. Pietrucha, K. 2005. Changes in denaturation and rheological properties of collagen-hyaluronic acid scaffolds as a result of temperature dependencies. *Int. J. Biol. Macromol.* 36:299–304.
49. Samouillan, V., A. Lamure, and C. Lacabanne. 2000. Dielectric relaxations of collagen and elastin in the dehydrated state. *Chem. Phys.* 255:259–271.
50. Wang, C. H. 2004. The principle of micro thermal analysis using atomic force microscope. *Thermochim. Acta.* 423:89–97.
51. Fenwick, O., L. Bozec, …, F. Cacialli. 2009. Thermochemical nanopatterning of organic semiconductors. *Nat. Nanotechnol.* 4:664–668.
52. Glimcher, M. J., and S. M. Krane. 1968. A treatise on collagen. *In* Biology of Collagen. G. N. Ramachandran and B. S. Gould, editors. Academic Press, New York. 67.
53. Nesbitt, S. A., and M. A. Horton. 1997. Trafficking of matrix collagens through bone-resorbing osteoclasts. *Science.* 276:266–269.

54. Nesbitt, S. A., and M. A. Horton. 2003. Fluorescence imaging of bone-resorbing osteoclasts by confocal microscopy. *Methods Mol. Med.* 80:259–281.

55. Bonar, L. C., and M. J. Glimcher. 1970. Thermal denaturation of mineralized and demineralized bone collagens. *J. Ultrastruct. Res.* 32:545–548.

56. Augustin, G., S. Davila, …, A. Antabak. 2008. Thermal osteonecrosis and bone drilling parameters revisited. *Arch. Orthop. Trauma Surg.* 128:71–77.

57. Eriksson, R. A., T. Albrektsson, and B. Magnusson. 1984. Assessment of bone viability after heat trauma. A histological, histochemical and vital microscopic study in the rabbit. *Scand. J. Plast. Reconstr. Surg.* 18:261–268.